# Design of Dual Rotors Switched Reluctance Motor

H. Chen, T. Xu and X. Liu
China University of Mining & Technology
Xuzhou, 21116, China
hchen@cumt.edu.cn

***Abstract*—This paper presents a mathematical model of the dual rotors switched reluctance motor. The magnetic flux density, magnetic energy storage, magnetic flux and magnetic flux linkage are described. The pictures of magnetic-flux paths distribution and magnetic flux density at different position are given. This study achieves optimization in structure are based on the present model.**

*Index Terms*—**Switched Reluctance, motor design, dual rotors.**

## I. Introduction

Switched reluctance motor (SRM) drive has a lot advantages and has a wide range of industrial applications [1]-[5]. Features like enhancing the reliability, reducing the noise and vibration [6]-[8] contribute significantly to the generalized applications of switched reluctance motor drive in industries.

In this paper, a dual rotors switched reluctance motor is designed by using finite-element method (FEM). Calculation and analysis of the electromagnetic torque have been performed. The flux distributions are obtained. The optimization in structure and geometry size is studied with the proposed model.

## II. Model For Dual Rotors Switched Reluctance Motor

As shown in Fig.1, there are one stator, the inner rotor, the outer rotor, the stator winding, the inner rotor winding, inner airgap and outer airgap in the dual rotors switched reluctance motor.

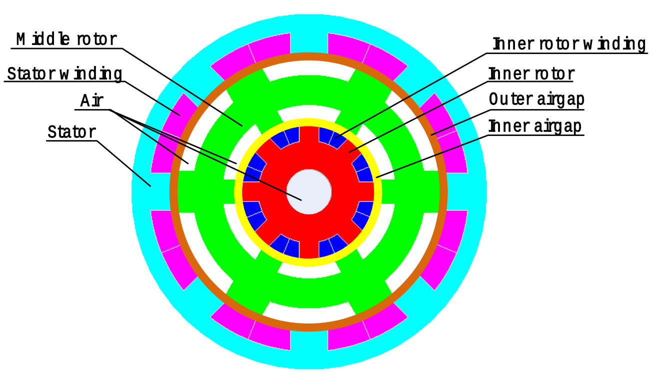


Fig. 1. Section of the dual rotors switched reluctance motor.

The following assumptions based on experience as well as the experiment are proposed for the present motor model.

1) Ignoring end effects and the magnetic field is axially uniform distribution. The magnetic vector potential $\vec{A}$ and current density $\vec{J}$ only have the *z* coordinate axial component of $\vec{A}_z$ and $\vec{J}_z$, so the magnetic flux density only have the components of $\vec{B}_x$ and $\vec{B}_y$.

2) The magnetic field is limited only to the internal motor. The internal boundary of the rotor and the external boundary of the stator are considered to be the zero vector magnetic potential line.

3) Neglecting hysteresis effect, the magnetization curve of the material of iron core is considered to be a single value.

4) Excluding the eddy current effect of the alternating magnetic field in the conductive materials, so that the magnetic field of the dual rotors switched reluctance motor can be used as a nonlinear and seemingly stable magnetic field.

The external motor is as follows,

$$\begin{cases} \dfrac{\partial}{\partial x}\left(\dfrac{1}{\mu}\dfrac{\partial \vec{A}_{z1}}{\partial x}\right)+\dfrac{\partial}{\partial y}\left(\dfrac{1}{\mu}\dfrac{\partial \vec{A}_{z1}}{\partial y}\right)=-\vec{J}_{z1} \\ \vec{A}_{z1}\,|_{\Gamma_1,\Gamma_2}=0 \end{cases} \tag{1}$$

and the internal motor is as follows,

$$\begin{cases} \dfrac{\partial}{\partial x}\left(\dfrac{1}{\mu}\dfrac{\partial \vec{A}_{z2}}{\partial x}\right)+\dfrac{\partial}{\partial y}\left(\dfrac{1}{\mu}\dfrac{\partial \vec{A}_{z2}}{\partial y}\right)=-\vec{J}_{z2} \\ \vec{A}_{z2}\,|_{\Gamma_3,\Gamma_4}=0 \end{cases} \tag{2}$$

where $\Gamma_1,\Gamma_2$ are respectively the outer circumference of the stator and the inner circumference of the middle rotor, $\Gamma_3,\Gamma_4$ are respectively the outer circumference of middle rotor and the inner circumference of the inner rotor, $\vec{J}_{z1}$ is the current density of the stator winding, $\vec{J}_{z2}$ is the current density of the inner rotor winding, $\vec{A}_{z1}$ and $\vec{A}_{z2}$ are the *z* coordinate axial component of the magnetic vector potential, $\mu$ is permeability of material.

The magnetic flux density is

$$\vec{B}=\nabla\times\vec{A}=x\frac{\partial \vec{A}}{\partial y}-y\frac{\partial \vec{A}}{\partial x} \tag{3}$$

The magnetic energy storage density is described as

$$W_m=\frac{l}{2}\sum_{e=1}^{E}\int_{\Omega^e} w_m d\Omega=\frac{l}{2}\sum_{e=1}^{E}\int_{\Omega^e}\left[\int_0^B \vec{H}d\vec{B}\right]d\Omega \tag{4}$$

where $\Omega$ is the volume of the motor, $\vec{H}$ is the magnetic field intensity.

## III. Analysis

The two-dimensional finite element mesh on the motor is shown in Fig.2, while a) mesh on section of the motor, b) subdivision mesh on airgap. $\theta_1$ is the position angle between middle rotor and stator; $\theta_2$ is the position angle between middle rotor and inner rotor. The magnetic-flux paths distribution is described in Fig. 3, while, a) $\theta_1 = 0^\circ, \theta_2 = 0^\circ$, b) $\theta_1 = 60^\circ, \theta_2 = 60^\circ$. The magnetic flux density is shown in Fig. 4, while, a) $\theta_1 = 0^\circ, \theta_2 = 0^\circ$, b) $\theta_1 = 60^\circ$, $\theta_2 = 60^\circ$. Fig. 5 gives the calculated four phase windings current of stator and Fig. 6 gives the calculated four phase windings current of inner rotor. The calculated magnetic flux of the external motor is shown in Fig. 7, and the calculated magnetic flux of the internal motor is shown in Fig. 8. The calculated torque of middle rotor is also shown in Fig. 9. The optimization in structure and geometry size is studied with the proposed model.

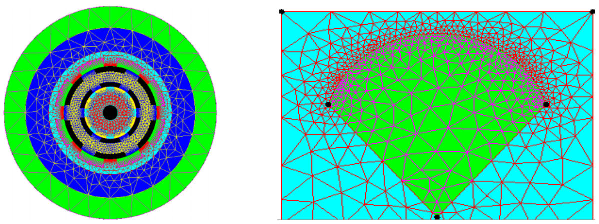

a) section b) airgap

Fig. 2. Two-dimensional finite element mesh.

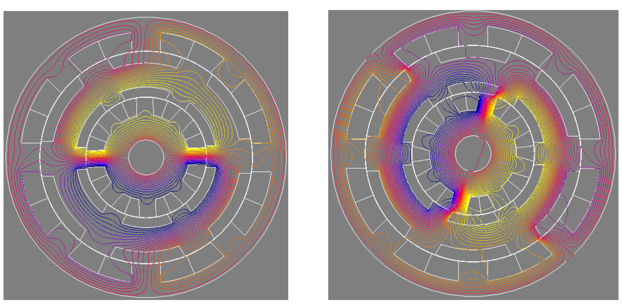

a) $\theta_1 = 0^\circ$, $\theta_2 = 0^\circ$ b) $\theta_1 = 60^\circ$, $\theta_2 = 60^\circ$

Fig. 3. Magnetic-flux paths distribution.

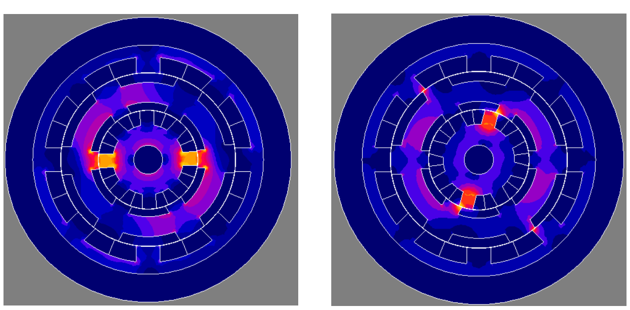

a) $\theta_1 = 0^\circ$, $\theta_2 = 0^\circ$ b) $\theta_1 = 60^\circ$, $\theta_2 = 60^\circ$

Fig. 4. Magnetic flux density.

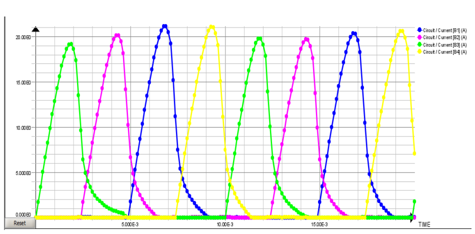

Fig. 5. Calculated four phase windings current of stator.

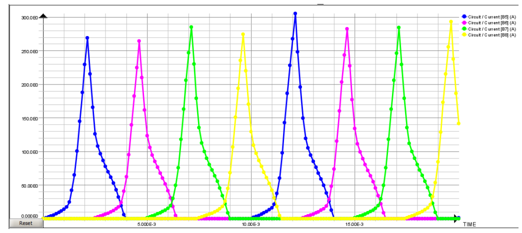

Fig. 6. Calculated four phase windings current of inner rotor.

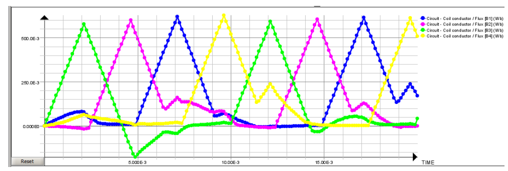

Fig. 7. Calculated magnetic flux of the external motor.

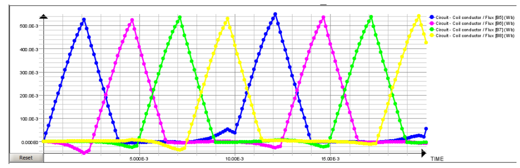

Fig. 8. Calculated magnetic flux of the internal motor.

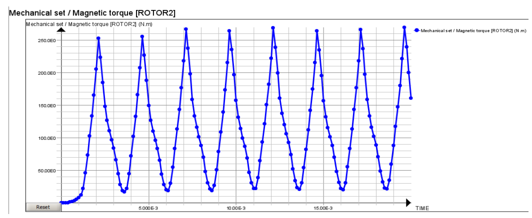


Fig. 9. Calculated torque of middle rotor.

## IV. Conclusion

In this paper, a model for dual rotors switched reluctance motor has been introduced. This model can optimize structure and geometry size of the motor. Considering the limitation of stator outer diameter and the limitation of inner rotor inner diameter, the configuration intensity and manufacture techniques, the final geometry size can be designed.

## References


[1] H. J. Chen et al., "A new analytical model for switched reluctance motors," *IEEE Trans. on Magnetics*, vol. 45, no. 8, pp. 3107–3113, Aug. 2009.

[2] Y. Hasegawa, K. Nakamura and O. Ichinokura, "Optimization of a switched reluctance motor made of permendur," *IEEE Trans. on Magnetics*, vol.46, no.6, pp.1311–1314, June 2010.

[3] .G. J. Li, J. Ojeda, E. Hoang, M. Lecrivain, and M. Gabsi, "Comparative studies between classical and mutually coupled switched reluctance motors using thermal-electromagnetic analysis for driving cycles," *IEEE Trans. on Magnetics*, vol.47, no.4, pp.839-861, April 2011.

[4] K. Lu, U. Jakobsen, and P. O. Rasmussen, "Single-phase hybrid switched reluctance motor for low-power low-cost applications," *IEEE Trans. on Magnetics*, vol.47, no.10, pp.3288-3291, Oct. 2011.

[5] Z. Zhang, N. C. Cheung, K. W. E. Cheng, X. D. Xue, and J. K. Lin, "Longitudinal and transversal end-effects analysis of linear switched reluctance motor," *IEEE Trans. on Magnetics*, vol.47, no.10, pp.3979-3982, Oct. 2011.

[6] D.G. Dorrell and C. Cossar, "A vibration-based condition monitoring system for switched reluctance machine rotor eccentricity detection," IEEE Trans. on Magnetics, vol.44, no.9, pp.2204 - 2214, Sept. 2008.

[7] J. Li, X. Song and Y. Cho, "Comparison of 12/8 and 6/4 switched reluctance motor: noise and vibration aspects," IEEE Trans. on Magnetics, vol.44, no.11, pp.4131-4134, Nov. 2008.

[8] J. Li and Y. Cho, "Investigation into reduction of vibration and acoustic noise in switched reluctance motors in radial force excitation and frame transfer function aspects," IEEE Trans. on Magnetics, vol.45, no.10, pp.4664 - 4667, Oct. 2009.